



Coupled Problem of Thermoelasticity for Multilayered Spheres with Time-Dependent Boundary Conditions

Zong-Yi Lee

Assistant Professor, Department of Mechanical Engineering, Hsiuping Institute of Technology Taichung, Taiwan 412, R.O.C., zylee@mail.hit.edu.tw

Follow this and additional works at: <https://jmstt.ntou.edu.tw/journal>



Part of the [Mechanical Engineering Commons](#)

Recommended Citation

Lee, Zong-Yi (2004) "Coupled Problem of Thermoelasticity for Multilayered Spheres with Time-Dependent Boundary Conditions," *Journal of Marine Science and Technology*. Vol. 12: Iss. 2, Article 4.

DOI: 10.51400/2709-6998.2225

Available at: <https://jmstt.ntou.edu.tw/journal/vol12/iss2/4>

This Research Article is brought to you for free and open access by Journal of Marine Science and Technology. It has been accepted for inclusion in Journal of Marine Science and Technology by an authorized editor of Journal of Marine Science and Technology.

COUPLED PROBLEM OF THERMOELASTICITY FOR MULTILAYERED SPHERES WITH TIME-DEPENDENT BOUNDARY CONDITIONS

Zong-Yi Lee

Key words: multilayered spheres, laplace transform, similarity transformation.

ABSTRACT

This paper deals with quasi-static coupled thermoelastic problems for multilayered spheres. Using the Laplace transform with respect to time, the general solutions of the governing equations are obtained in transform domain. The solution is obtained by using the matrix similarity transformation and inverse Laplace transform. We obtain solutions for the temperature and thermal deformation distributions for a transient state. It is demonstrated that the computational procedures established in this paper are capable of solving the generalized thermoelasticity problem of multilayered spheres.

INTRODUCTION

The increasing use of composite materials in engineering application has resulted in considerable research activity in this area in recent years. An understanding of thermally induced stresses in isotropic bodies is essential for a comprehensive study of their response due to an exposure to a temperature field, which may in turn occur in service or during the manufacturing stages. While the deformation and stress fields in a shell caused by thermal effects have commonly been obtained on the basis of uncoupled thermoelasticity theory, the thermo-mechanical coupling effect is included in the present study.

Vollbrecht [9] has analysed the stresses in both cylindrical and spherical walls subjected to internal pressure and stationary heat flow. Kandil [5] has studied the effect of steady-state temperature and pressure gradient on compound cylinders fitted together by shrink fit. Ghosn and Sabbaghian [3] investigated a one-dimensional axisymmetric quasi-static coupled

thermoelasticity problem. The solution technique uses Laplace transform. The inversion to real domain is obtained by means of Cauchy's theorem of residues and the convolution theorem. Sherief and Anwar [6] discussed the problem of an infinitely long elastic circular cylinder whose inner and outer surfaces are subjected to known temperature and are traction free. They have neglected both the inertia terms and the relaxation effects. Takeuti and Furukawa [7] discussed the thermal shock problem in a plate; they included the inertia and thermoelastic coupling terms in the governing equation and obtained the exact solution for the thermal shock problem of a plate. Chen and Yang [1] discussed the transient response of one-dimensional quasi-static coupled thermoelasticity problems of an infinitely long cylinder composed of two different materials. They applied the Laplace transform with respect to time and used the Fourier series and matrix operations to obtain the solution. Chen and Chen [2] presented a new numerical technique hybrid numerical method for the problem of a transient linear heat conduction system. They applied the Laplace transform to remove the time-dependence from the governing equations and boundary conditions, and solved the transformed equations with the finite element and finite difference method. Jane and Lee [4] considered the same problem by using the Laplace transform and the finite difference method. The cylinder was composed of multilayers of different materials. There is no limit to the number of annular layers of the cylinder in the computational procedures. Laplace transform and finite difference methods were used to analyze problems. They obtained solutions for the temperature and thermal stress distributions in a transient state.

In this paper, the one-dimensional quasi-static coupled thermoelastic problem of a multilayered sphere with time-dependent boundary conditions is considered. The medium is without body forces and heat generation. Laplace transform and finite difference methods are used, which are quite effective and powerful, to obtain

Paper Submitted 01/19/04, Accepted 04/13/04. Author for Correspondence: Zong-Yi Lee. E-mail: zylee@mail.hit.edu.tw.

**Assistant Professor, Department of Mechanical Engineering, Hsiuping Institute of Technology Taichung, Taiwan 412, R.O.C.*

solutions of a wide range of transient thermal stress.

FORMULATION

This work deals with the thermo-mechanically coupled problems of multilayered spheres using the quasi-static approach. The problems possess the spherical symmetry with the following additional assumption: (1) Materials in each layer is assumed to be homogeneous, isotropic and linearly thermoelastic. (2) Deformation is small. (3) The composite sphere is constructed of multilayer laminates bonded perfectly together. (4) All physical quantities are assumed to be functions of the radial coordinate and time only. (5) The medium is initially undisturbed, traction free, and without body forces and internal heat sources.

The layered sphere to be analyzed is shown in Fig. 1. The transient heat conduction equation for the *i*th layer in dimensional form can be written as

$$k[\frac{\partial^2}{\partial r^{*2}} + \frac{2}{r^*} \frac{\partial}{\partial r^*}] \bar{\Theta} = \rho C_v \frac{\partial \bar{\Theta}}{\partial \tau} + \Theta_0 \beta \frac{\partial}{\partial r^*} (\frac{\partial U}{\partial \tau}) + \Theta_0 \beta \frac{1}{r^*} (\frac{\partial U}{\partial \tau}) \tag{1}$$

where $\bar{\Theta} = \Theta - \Theta_0$, $\beta = \frac{E\alpha}{1-\nu}$

Θ_0 is the referential temperature

If body forces are absent, the equation of equilibrium for a sphere along the radial direction can be written as

$$\frac{\partial^2 U}{\partial r^{*2}} + \frac{2}{r^*} \frac{\partial U}{\partial r^*} - \frac{1}{r^{*2}} U = \frac{1+\nu}{1-\nu} \alpha \frac{\partial \bar{\Theta}}{\partial r^*} \tag{2}$$

The stress-displacement relations are

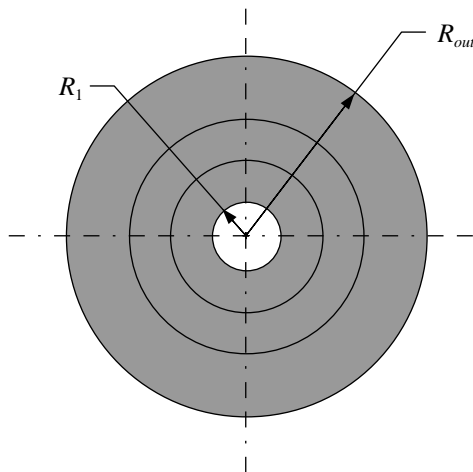


Fig. 1. Physical model and system coordinates for a multilayered spheres.

$$\sigma_{ri}^* = \frac{E}{(1+\nu)(1-2\nu)} [(1-\nu) \frac{\partial U}{\partial r^*} + 2\nu \frac{U}{r^*} - \alpha(1+\nu)(\Theta - \Theta_0)] \tag{3}$$

$$\sigma_{\theta i}^* = \frac{E}{(1+\nu)(1-2\nu)} [\nu \frac{\partial U}{\partial r^*} + \frac{U}{r^*} - \alpha(1+\nu)(\Theta - \Theta_0)] \tag{4}$$

Let the boundary surfaces of the composite sphere be subjected to the initial and time-dependent boundary conditions given below

$$U = \dot{U} = \bar{\Theta} = \dot{\bar{\Theta}} = 0 \quad \text{at } \tau = 0$$

$$\sigma_r^*(r^*, \tau) = p(\tau), \Theta_1 - \Theta_0 = f(\tau) \quad \text{at } r^* = R_1$$

$$\sigma_r^*(r^*, \tau) = 0, -k \frac{\partial \bar{\Theta}}{\partial r^*} = h(\Theta - \Theta_\infty) \quad \text{at } r^* = R_{out}$$

At the interface between two adjacent layers, the following matching conditions must be satisfied:

$$U_i(r^*, \tau) = U_{i+1}(r^*, \tau) \quad r^* = r_{i+1}^*$$

$$\sigma_{ri}^*(r^*, \tau) = \sigma_{ri+1}^*(r^*, \tau) \quad r^* = r_{i+1}^*$$

$$q_i = q_{i+1} \quad r^* = r_{i+1}^*$$

$$\bar{\Theta}_i(r^*, \tau) = \bar{\Theta}_{i+1}(r^*, \tau) \quad r^* = r_{i+1}^*$$

$i = 1, 2, \dots, m - 1$ layer

The non-dimensional variables are defined as follows:

$$T = (\Theta - \Theta_0) / \Theta_0 = \bar{\Theta} / \Theta_0$$

$$r = r^* / R_1$$

$$t = (\frac{k}{\rho C_v}) \tau / R_1^2$$

$$u = U (\frac{\beta}{\rho C_v}) / R_1$$

$$a_i = (\frac{k}{\rho C_{v_i}}) / (\frac{k}{\rho C_{v_1}})$$

$$\sigma_{ri} = \sigma_{ri}^* / (\beta_1 \Theta_0)$$

$$\sigma_{\theta i} = \sigma_{\theta i}^* / (\beta_1 \Theta_0)$$

$${}_3Q_i = [\frac{E\alpha}{(1-2\nu)}]_i / \beta_1$$

$${}_3R_i = [\frac{E\alpha}{(1-2\nu)}]_i / \beta_1$$

$$\begin{aligned}
{}_1Q_i &= \left[\frac{E(1-\nu)}{(1+\nu)(1-2\nu)} \right]_i / [\beta_1 \left(\frac{\beta}{\rho C_{\nu i}} \right) \Theta_0] \\
{}_2Q_i &= \left[\frac{2E\nu}{(1+\nu)(1-2\nu)} \right]_i / [\beta_1 \left(\frac{\beta}{\rho C_{\nu i}} \right) \Theta_0] \\
{}_1R_i &= \left[\frac{E\nu}{(1+\nu)(1-2\nu)} \right]_i / [\beta_1 \left(\frac{\beta}{\rho C_{\nu i}} \right) \Theta_0] \\
{}_2R_i &= \left[\frac{E}{(1+\nu)(1-2\nu)} \right]_i / [\beta_1 \left(\frac{\beta}{\rho C_{\nu i}} \right) \Theta_0] \\
g_i &= \left[\left(\frac{\beta}{\rho C_{\nu i}} \right) \alpha(1+\nu) \right]_i \Theta_0
\end{aligned} \quad (5)$$

Substituting the nondimensional quantities given in equation (5) into the governing equations (1)-(4), the governing equations and stress-displacement relations assume the following nondimensional form:

$$[a_i \left[\frac{\partial^2}{\partial r^2} + \frac{2}{r} \frac{\partial}{\partial r} \right] - \frac{\partial}{\partial t}] T = \frac{\partial}{\partial r} \left(\frac{\partial u}{\partial t} \right) + \frac{1}{r} \left(\frac{\partial u}{\partial t} \right) \quad (6)$$

$$\frac{\partial^2 u}{\partial r^2} + \frac{2}{r} \frac{\partial u}{\partial r} - \frac{u}{r^2} = g_i \frac{\partial T}{\partial r} \quad (7)$$

$$\sigma_{ri} = {}_1Q_i \frac{\partial u}{\partial r} + {}_2Q_i \frac{u}{r} - {}_3Q_i T \quad (8)$$

$$\sigma_{\theta i} = {}_1R_i \frac{\partial u}{\partial r} + {}_2R_i \frac{u}{r} - {}_3R_i T \quad (9)$$

The nondimensional boundary and interface conditions can be written as:

1. Boundary conditions

$$\sigma_r(r, t) = \frac{p(t)}{\beta_1 \Theta_0}, \quad T_1 = f(t) / \Theta_0 \quad \text{at } r = r_1$$

$$\sigma_r(r, t) = 0, \quad -k \frac{\partial T}{\partial r} = h(T - T_\infty) \quad \text{at } r = r_{out}$$

2. Interface conditions

$$u_i(r, t) = u_{i+1}(r, t) \quad r = r_{i+1}$$

$$\sigma_{ri}(r, t) = \sigma_{ri+1}(r, t) \quad r = r_{i+1}$$

$$q_i = q_{i+1} \quad r = r_{i+1}$$

$$T_i(r, t) = T_{i+1}(r, t) \quad r = r_{i+1}$$

$i = 1, 2, \dots, m-1$ layer

NUMERICAL PROCEDURE AND SOLUTION

Applying central differences in equations (6), (7), (8) and (9), we obtain the following discretized equations:

$$a_i \left(\frac{T_{j+1} - 2T_j + T_{j-1}}{(\Delta r_i)^2} + \frac{1}{r_j} \frac{T_{j+1} - T_{j-1}}{\Delta r_i} \right) - \frac{\partial T_j}{\partial t}$$

$$= \frac{1}{r_j} \frac{\partial u_j}{\partial t} + \frac{\left(\frac{\partial u}{\partial t} \right)_{j+1} - \left(\frac{\partial u}{\partial t} \right)_{j-1}}{2\Delta r_i} \quad (10)$$

$$\begin{aligned}
& \frac{u_{j+1} - 2u_j + u_{j-1}}{(\Delta r_i)^2} + \frac{1}{r_j} \frac{u_{j+1} - u_{j-1}}{\Delta r_i} - \frac{1}{r_j^2} u_j \\
& = g_i \frac{T_{j+1} - T_{j-1}}{2\Delta r_i}
\end{aligned} \quad (11)$$

$$\sigma_{ri} = {}_1Q_i \frac{u_{j+1} - u_{j-1}}{2\Delta r_i} + {}_2Q_i \frac{u_j}{r_j} - {}_3Q_i T_j \quad (12)$$

$$\sigma_{\theta i} = {}_1R_i \frac{u_{j+1} - u_{j-1}}{2\Delta r_i} + {}_2R_i \frac{u_j}{r_j} - {}_3R_i T_j \quad (13)$$

where $\Delta r_i = (r_{i+1} - r_i) / (n - 1)$ and n is number of grid point for each layer

The Laplace transform of a function $\Phi(t)$ and its inverse are defined by

$$\overline{\Phi}(s) = L[\Phi(t)] = \int_0^\infty e^{-st} \Phi(t) dt$$

$$\Phi(t) = L^{-1}[\overline{\Phi}(s)] = \frac{1}{2\pi i} \int_{c-i\infty}^{c+i\infty} e^{st} \overline{\Phi}(s) ds$$

Taking the Laplace transform for equations (10), (11), (12) and (13), we obtain the following equations:

$$\begin{aligned}
& a_i \left(\frac{\overline{T}_{j+1} - 2\overline{T}_j + \overline{T}_{j-1}}{(\Delta r_i)^2} + \frac{1}{r_j} \frac{\overline{T}_{j+1} - \overline{T}_{j-1}}{\Delta r_i} \right) \\
& - (T_{j, in} + s \overline{T}_j) \\
& = \frac{1}{r_j} (u_{j, in} + s \overline{u}_j) + \frac{1}{2\Delta r_i} [(u_{j+1, in} + s \overline{u}_{j+1}) \\
& - (u_{j-1, in} + s \overline{u}_{j-1})]
\end{aligned} \quad (14)$$

$$\begin{aligned}
& \frac{\overline{u}_{j-1} - 2\overline{u}_j + \overline{u}_{j-1}}{(\Delta r_i)^2} + \frac{1}{r_j} \frac{\overline{u}_{j+1} - \overline{u}_{j-1}}{\Delta r_i} - \frac{1}{r_j^2} \overline{u}_j \\
& = g_i \frac{\overline{T}_{j+1} - \overline{T}_{j-1}}{2\Delta r_i}
\end{aligned} \quad (15)$$

Let the surface of the sphere inner surface be traction free and subject to a time-dependent temperature. After taking Laplace transforms, the boundary conditions in the transformed domain become

$$\overline{\sigma}_r(r, s) = \frac{\overline{p}(s)}{\beta_1 \Theta_0}, \quad \overline{T}_1 = \overline{f}(s) / \Theta_0 \quad \text{at } r = r_1$$

$$\overline{\sigma}_r(r, s) = 0, \quad -k \frac{\partial \overline{T}}{\partial r} = h(\overline{T} - \overline{T}_\infty) \quad \text{at } r = r_{out} \quad (16)$$

$$\begin{aligned}
H_j &= \frac{g_i}{2\Delta r_i} \\
K_j &= \frac{1}{(\Delta r_i)^2} - \frac{2}{r_j} \frac{1}{2\Delta r_i} \\
L_j &= -\frac{2}{(\Delta r_i)^2} + \frac{1}{r_j^2} \\
M_j &= \frac{1}{(\Delta r_i)^2} + \frac{1}{r_j} \frac{1}{\Delta r_i} \\
\bar{V}_j &= 0 \\
H_N &= \frac{g_m}{2\Delta r_m} \\
I_N &= \frac{3Q_m}{1Q_m} \left(\frac{2}{r_m} + \frac{2}{\Delta r_m} \right) \\
K_N &= \frac{2}{(\Delta r_m)^2} \\
L_N &= \frac{2Q_m}{1Q_m} \left(\frac{-2}{r_m \Delta r_m} - \frac{2}{r_m^2} \right) - \frac{2}{(\Delta r_m)^2} - \frac{1}{r_m^2} \\
\bar{V}_N &= -\frac{g_m}{2\Delta r_m} T_{N+1}
\end{aligned}$$

Equations (18) and (19) can be rewritten in the following matrix forms

$$[\mathbf{M}] - s[\mathbf{I}] \{ \bar{T}_j \} + s[\mathbf{N}] \{ \bar{u}_j \} = \{ \bar{G}_j \} \quad (20)$$

$$[\mathbf{R}] \{ \bar{T}_j \} + [\mathbf{Q}] \{ \bar{u}_j \} = \{ \bar{V} \} \quad (21)$$

where the matrices $[\mathbf{M}]$, $[\mathbf{N}]$, $[\mathbf{R}]$ and $[\mathbf{Q}]$ are the corresponding matrices in equations (18) and (19). Substituting equation (21) into (20), we have

$$[\mathbf{A}] - s[\mathbf{I}] \{ \bar{T}_j \} = \{ \bar{F}_j \} \quad (22)$$

where

$$\begin{aligned}
[\mathbf{A}] &= \{ [\mathbf{N}]^{-1} + [\mathbf{Q}]^{-1}[\mathbf{R}] \}^{-1} [\mathbf{N}]^{-1} [\mathbf{M}] \\
[\mathbf{F}_j] &= \{ [\mathbf{N}]^{-1} + [\mathbf{Q}]^{-1}[\mathbf{R}] \}^{-1} \{ [\mathbf{N}]^{-1} [\bar{G}_j] - s[\mathbf{Q}]^{-1} [\bar{V}] \}
\end{aligned}$$

Since the $(N \times N)$ matrix $[\mathbf{A}]$ is a nonsingular real matrix, the matrix $[\mathbf{A}]$ possesses a set of N linearly independent eigenvectors, hence the matrix $[\mathbf{A}]$ is diagonalizable. Therefore, there exists a nonsingular transition matrix $[\mathbf{P}]$ such that $[\mathbf{P}]^{-1}[\mathbf{A}][\mathbf{P}] = \text{diag} [\mathbf{A}]$, that is, the matrices $[\mathbf{A}]$ and $\text{diag} [\mathbf{A}]$ are similar, where the matrix $\text{diag} [\mathbf{A}]$ is defined as

$$\text{diag} [\mathbf{A}] = \begin{bmatrix} \lambda_1 & & & \\ & \lambda_1 & & \\ & & \ddots & \\ & & & \lambda_N \end{bmatrix} \quad (23)$$

where $\lambda_j (j = 1, 2, \dots, N)$ are the eigenvalues of matrix $[\mathbf{A}]$.

Substituting equation (23) into (22), we obtain the equation

$$\{ [\mathbf{P}]^{-1}[\mathbf{A}][\mathbf{P}] - s[\mathbf{P}]^{-1}[\mathbf{I}][\mathbf{P}] \} [\mathbf{P}]^{-1} \{ \bar{T}_j \} = [\mathbf{P}]^{-1} \{ \bar{F}_j \} \quad (24)$$

Equation (24) can be rewritten as

$$\{ \text{diag}[\mathbf{A}] - s[\mathbf{I}] \} \{ \bar{T}_j^* \} = \{ \bar{F}_j^* \} \quad (25)$$

where

$$\bar{T}_j^* = [\mathbf{P}]^{-1} \{ \bar{T}_j \}$$

$$\bar{F}_j^* = [\mathbf{P}]^{-1} \{ \bar{F}_j \}$$

From equation (25), the following solutions can be obtained immediately.

$$\bar{T}_j^* = \frac{\bar{F}_j^*}{\lambda_j - s} \quad j = 1, 2, \dots, N \quad (26)$$

By applying the inverse Laplace transform to equation (26), we obtain the solution for T_j^* . After we have obtained T_j^* , we can then use equations (27) and (28) given below to obtain the solutions for T_j and u_j .

$$\{ T_j \} = [\mathbf{P}] \{ T_j^* \} \quad (27)$$

$$\{ u_j \} = [\mathbf{Q}]^{-1} [\bar{V}] - [\mathbf{Q}]^{-1} [\mathbf{R}] \{ T_j \} \quad (28)$$

Substituting T_j and u_j into equations (8) and (9), we obtain the radial and circumferential stresses.

NUMERICAL RESULTS AND DISCUSSIONS

In this study, we present some numerical results for the temperature distributions in multilayered composite spheres, subjected to the considered boundary conditions and the resulting displacement and thermal stresses. For the multilayered spheres, the geometry and material quantities of the sphere are shown in Table 1. The table 2 and table 3 show the computation time for different number of finite difference grid points. The inner and outer radii of the sphere are assumed to be 1.0 and 4.5, respectively. The boundary conditions at inner and outer surfaces are assumed to be $f(t)$ and convective respectively. Each layer is assumed to have a different thickness (nondimensional thickness of each layer is taken for $\Delta h_1 = 1$, $\Delta h_2 = 1$, and $\Delta h_3 = 1.5$, respectively). In all the figures, the grid points assumed

Table 1. The geometry and material constants of multilayered sphere ($R_{out} / R_1 = 4.5, h = 200 \frac{Watt}{m^2 \cdot K}, \Theta_0 = \Theta_\infty = 298 K$)

	layer 1 Titanium	layer 2 Al ₂ O ₃	layer 3 Steel(1025)
$E(\frac{N}{m^2})$	108E9	390E9	207E9
$k(\frac{Watt}{m \cdot K})$	20	6	17
ν	0.3	0.23	0.3
$\alpha(\frac{1}{K})$	11E-6	8E-6	11E-6
$\rho(\frac{kg}{m^3})$	4	3.99	7.8
$C_v(\frac{kJ}{kg \cdot K})$	0.4	1.25	0.48

Table 2. Computation time for coupled theory

	Grids = 69	Grids = 99	Grids = 129	Grids = 219
t = 1	3.21380	7.911376	12.76836	34.61978
t = 10	3.865558	8.23140	13.16894	36.70278
t = 30	7.85129	16.24336	27.30927	78.54294

(CPU P3_700, unit = second)

Table 3. Computation time for uncoupled theory

	Grids = 69	Grids = 99	Grids = 129	Grids = 219
t = 1	2.103024	4.065846	6.259000	17.57527
t = 10	2.633787	5.377733	8.762600	25.53672
t = 30	5.397762	10.96577	18.39645	54.08778

(CPU P3_700, unit = second)

219 ($N = 219$).

Fig. 2 shows water vapour temperature and pressure relation assumed for the inner boundary. The water vapour temperature and pressure data were obtained from a thermodynamic steam table [8]. Fig. 3 shows the temperature distributions with time. Fig. 4 shows the pressure distributions with time. Fig. 5a shows the temperature distributions along the radial direction and with time. Fig. 5b shows the temperature distributions with time and different radial locations. The temperature gradient varies in each layer because of the difference in the thermal conductivity coefficients. Fig. 6a shows the variation of the radial displacement as a function of the radial coordinate and time. Fig. 6b shows the displacement distributions with time and different radial locations. From these figures, we can

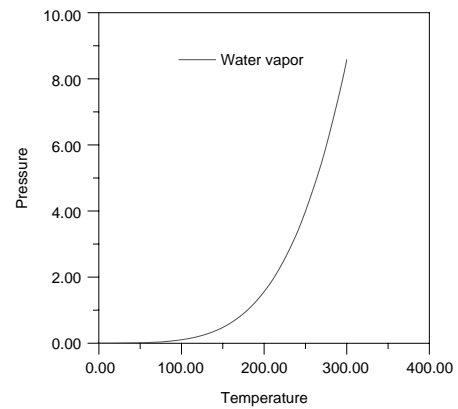


Fig. 2. Temperature and pressure relation in inner boundary (quality 90%) [9].

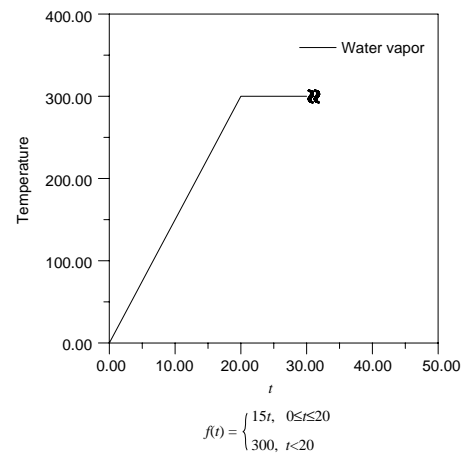


Fig. 3. Temperature distribution with time in inner boundary.

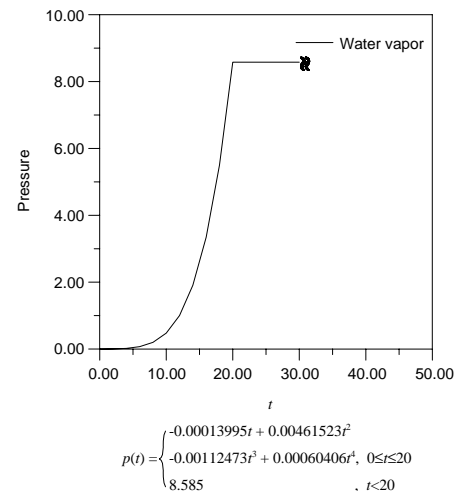


Fig. 4. Pressure distribution with time in inner boundary.

see where the maximum radial displacement may occur. Fig. 7a shows the thermal radial stress distribution σ_r along the radial direction and with time. Fig. 7b shows the thermal radial stress distribution σ_r with time and different radial locations. As expected, the circumferential stress distribution exhibits significant jumps at all interfaces as shown in Fig. 8a. These discontinuities are due to the differences in material properties such as the coefficient of linear thermal expansion and Young's

modulus. The circumferential stress varies characteristically in each layer in view of the occurrence of discontinuities at all interfaces shown in the Fig. 8a. Fig. 8b shows the circumferential stress distribution with time and different radial locations. In all the figures, the dotted lines express the results of uncoupled cases. It is obvious that there is distinct difference between the coupled and uncoupled treatment. From these figures, it should be concluded that the coupling

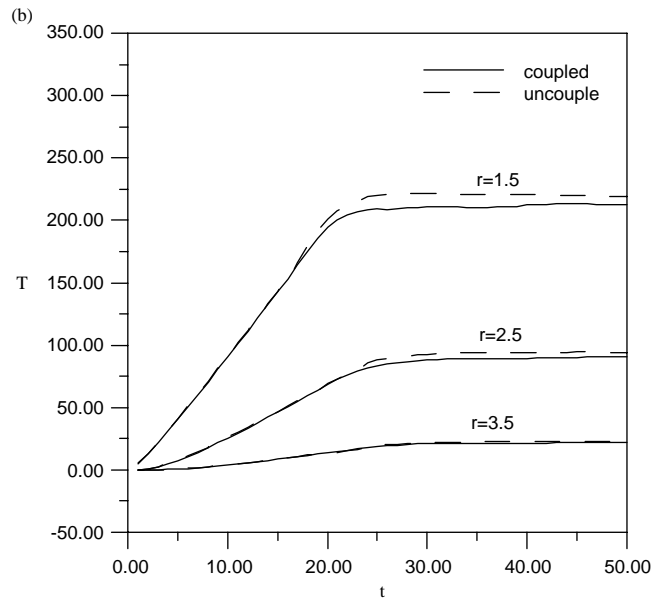
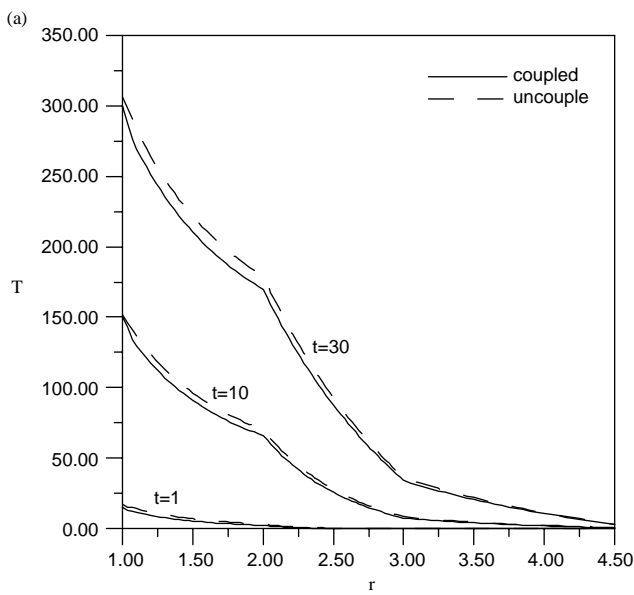


Fig. 5. (a) Temperature distribution along radial direction and different times, (b) Temperature distribution with time and different radial locations.

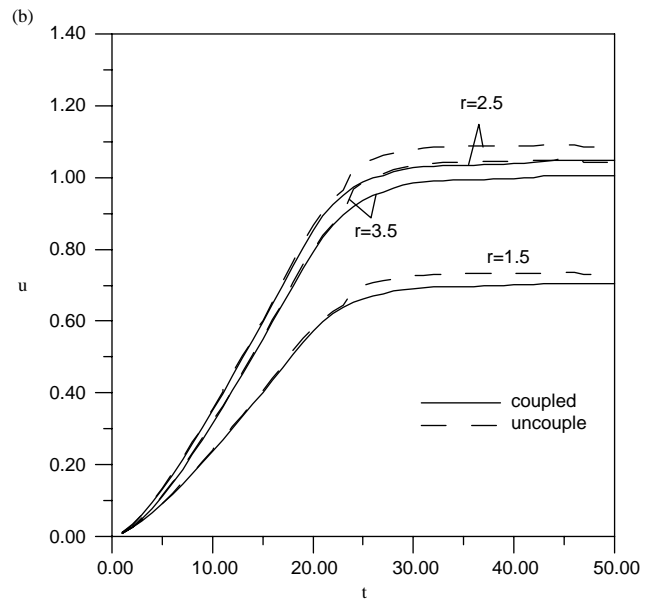
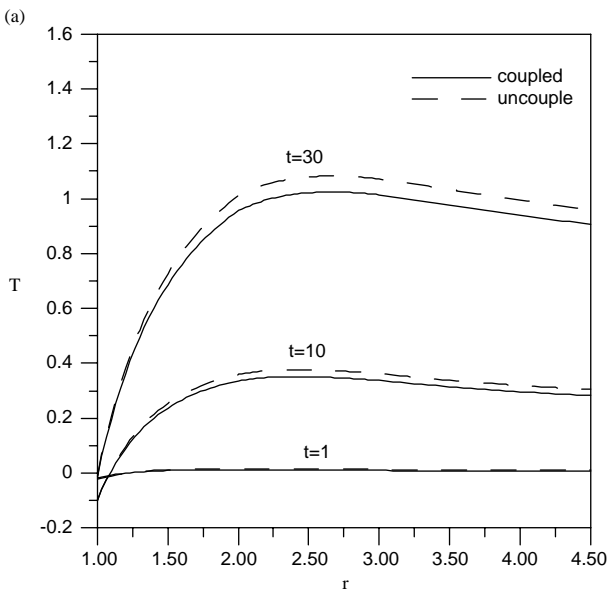


Fig. 6. (a) Radial displacement distribution along radial direction and different times, (b) Radial displacement distribution with time and different radial locations.

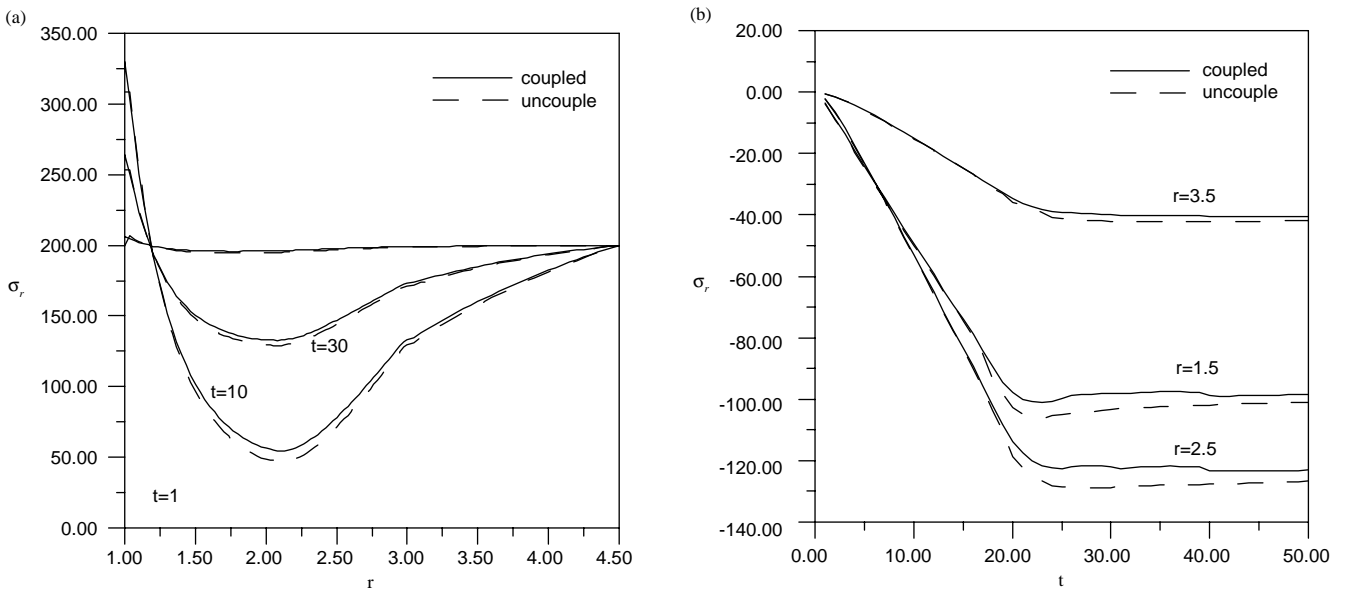


Fig. 7. (a) Radial stress distribution along radial direction and different times, (b) Radial stress distribution with time and different radial locations.

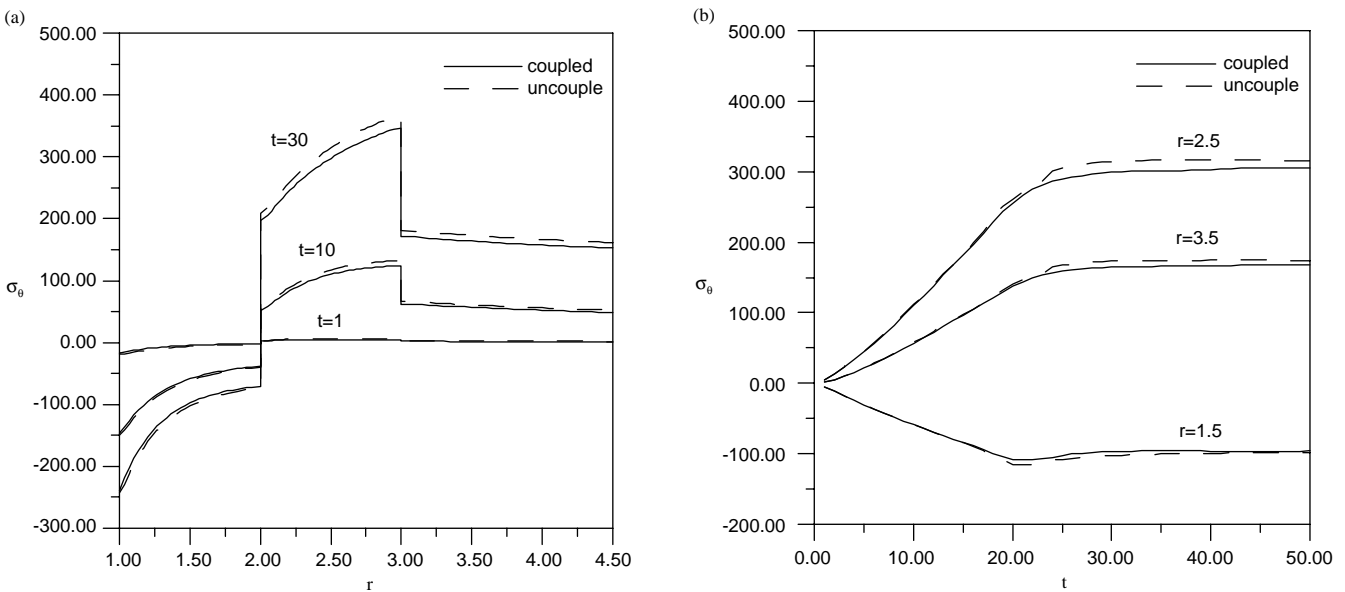


Fig. 8. (a) Circumferential stress along radial direction and different times, (b) Circumferential stress for time and different radial locations.

effect behaves as a clear lag.

CONCLUSIONS

In this study, numerical results for a multilayered sphere were calculated. The finite difference and Laplace transform methods were employed to obtain the numerical results. The temperature, displacement and thermal stress distributions were obtained which can be applied

to mechanical parts in precision measurement or design useful structural applications. The proposed method may be readily extended to solve a wide range of physical engineering problems.

NOMENCLATURE

ρ density
 C_v specific heat

k	thermal conductivity
α	linear thermal expansion coefficient
E	Young's modulus
ν	Poisson's ratio
Θ_0	reference temperature
h	convective heat transfer coefficient
q	heat flux in the radial direction
N	total number of grid point
$T_{j, in}$	initial condition
$u_{j, in}$	initial condition
Θ, T	dimensional and non-dimensional temperature
r^*, r	dimensional and non-dimensional radial coordinate
τ, t	dimensional and non-dimensional time ,
σ_r^*, σ_r	dimensional and non-dimensional radial stress
$\sigma_\theta^*, \sigma_\theta$	dimensional and non-dimensional circumferential stress
U, u	dimensional and non-dimensional radial component of displacement

REFERENCES

- Chen, C.K. and Yang, Y.C., "Thermoelastic Transient Response of an Infinitely Long Annular Cylinder Composed of Two Different Materials," *J. Eng. Sci.*, Vol. 24, pp. 569-581 (1986).
- Chen, C.K. and Chen, T.M., "New Hybrid Laplace Transform/Finite Element Method for Three-Dimensional Transient Heat Conduction Problem," *Int. J. Numerical Methods Engin.*, Vol. 32, No. 1, pp. 45-61 (1991).
- Ghosn, A.H. and Sabbaghian, M., "Quasi-Static Coupled Problems of Thermoelasticity for Cylindrical Regions," *J. Thermal Stresses*, Vol. 5, pp. 299-313 (1982).
- Jane, K.C. and Lee, Z.Y., "Thermoelastic Transient Response of an Infinitely Long Multilayered Cylinder," *Mech. Res. Comm.*, Vol. 26, No. 6, pp. 709-718 (1999).
- Kandil, A., "Investigation of Stress Analysis in Compound Cylinders Under High Pressure and Temperature," M. Sc. Thesis, CIT Helwan Univ., Egypt (1975).
- Sherief, H.H. and Anwar, M.N., "A Problem in Generalized Thermoelasticity for an Infinitely Long Annular Cylinder," *Int. J. Eng. Sci.*, Vol. 26, pp. 301-306 (1988).
- Takeuti, Y. and Furukawa, T., "Some Consideration on Thermal Shock Problem in a Plate," *J. Appl. Mech.*, Vol. 48, pp. 113-118 (1981).
- van Wylen, G.V., Sonntag, R., and Borgnakke, C., *Fundamentals of Classical Thermodynamics*, Fourth Edition, Wiley, New York (1994).
- Vollbrecht, H., "Stress in Cylindrical and Spherical Walls Subjected to Internal Pressure and Stationary Heat Flow," *Verfahrenstechnik*, Vol. 8, pp. 109-112 (1974).